Carbohydrate Polymers 118 (2015) 91–100

Contents lists available at ScienceDirect

Carbohydrate Polymers

journal homepage: www.elsevier.com/locate/carbpol

NMR characterization of cellulose acetate: Chemical shift assignments, substituent effects, and chemical shift additivity

Hiroyuki Kono*, Hisaho Hashimoto, Yuuichi Shimizu

Department of Science and Engineering for Materials, Tomakomai National College of Technology, Nishikioka 443, Tomakomai 059 1275, Hokkaido, Japan

ARTICLE INFO

Article history:
Received 16 September 2014
Received in revised form 24 October 2014
Accepted 8 November 2014
Available online 15 November 2014

Keywords:
Cellulose acetate
Chemical shift
Substituent effect
Substituent distribution

ABSTRACT

A series of cellulose acetates (CA) with degrees of substitution (DS) ranging from 2.92–0.92 dissolved in dimethylsulfoxide (DMSO)-d_6 and cellulose dissolved in tetrabutylammonium fluoride (TBAF)/DMSO-d_6 were investigated by two-dimensional NMR spectroscopy. The NMR spectroscopic analysis allowed the determination of the ^{1}H and ^{13}C NMR chemical shifts of the eight anhydroglucose units (AGUs) that contain CA: 2,3,6-tri-, 2,3-di-, 2,6-di-, 3,6-di-, 2-mono-, 3-mono-, 6-mono-, and unacetylated AGUs. A comparative analysis of the chemical shift data revealed the substituent effect of acetyl groups at the 2-, 3-, and 6-positions on the ^{1}H and ^{13}C nuclei in the same AGU. In addition, chemical shift additivity could be applied to the ^{1}H and ^{13}C chemical shifts of CA because the chemical shifts of the diacetylated and triacetylated AGUs could be almost completely explained by the acetyl substituent effects at the 2-, 3-, and 6-positions.

1. Introduction

From an analytical point of view, cellulose acetate (CA) is the simplest cellulose ester structure. CA is industrially produced from the esterification of the hydroxyl groups at the 2-, 3-, and 6-positions of the anhydroglucose units (AGUs) of cellulose with acetic anhydride in the presence of acetic acid as a solvent and concentrated sulfuric acid as an esterification catalyst (Malm, Tanghe, & Laird, 1946). The degree of substitution (DS), i.e., the average number of acetyl groups per AGU, ranges from 1.8 to 2.5 in the commercial acetone-soluble products. The properties of CA, such as solubility and viscosity, are closely related to the individual DS at the 2-, 3-, and 6-positions along the cellulose chains, as well as the overall DS (Fox, Li, Xu, & Edgar, 2011; Xu & Edgar, 2012).

In order to determine the CA structure, including the DS and substituent distribution at the monomer level, NMR spectroscopy is applied to get a first look into the individual DS. The CA chains are partially degraded by enzymes. The partial degradation of the CA chains results in a mixture of monomers and oligomers in different molecular ratios. Such mixtures have been separated and characterized in detail using various analytical techniques such as mass spectroscopy (Bashir, Critchley, & Derrick, 2001). Although this approach provides information on the monomer composition as well as the substituent distribution at the oligomeric level, the chemical heterogeneity of CA at the intact polymeric chain level is generally lost. As a new technique for obtaining the structural information of CA at the polymeric chain level, liquid chromatography using multi-step gradient separation has been used and allows the determination of the DS distribution of intact CA chains over a wide DS range of 1.5–2.9. Further, this technique reveals the chemical heterogeneity of the CA structure (Ghareeb & Radke, 2013).

As mentioned above, NMR spectroscopy has been frequently used to reveal the molecular structure of CA, including substituent distribution, DS, etc., because this method provides structural information at the polymer level without any pretreatments. The most well-known method, which was reported by Tezuka and Tsuchiya (1995), is the quantitative analysis of acetyl carbonyl carbons in CA samples, in which unsubstituted hydroxyl groups are perpropionylated by propionic anhydride prior to NMR analysis. The perpropionylated CA shows two sets of three well-resolved carbonyl carbon resonances attributed to the acetyl and propionyl groups substituted at the 2-, 3-, and 6-positions. Thus, the individual DS of CA can be estimated from the relative intensities of the integrals for the three acetyl carbonyl carbons. The perpropionylation of the unsubstituted hydroxyl groups of CA eliminates

Abbreviations: 1D, one-dimensional; 2D, two-dimensional; AGU, anhydroglucose unit; BBO, broadband observe; CA, cellulose acetate; CDCl3, chloroform-d; COSY, correlation spectroscopy; DMAP, *N*,*N*-dimethylaminopyridine; DMSO, dimethylsulfoxide; DS, degree of substitution; HSQC, heteronuclear single quantum coherence; Mn, molecular weight; NMR, nuclear magnetic resonance; TBAF, tetrabutylammonium fluoride; TOCSY, total correlation spectroscopy.

* Corresponding author. Tel.: +81 144 67 8036; fax: +81 144 67 8036.
E-mail address: kono@sem.tomakomai-ct.ac.jp (H. Kono).

http://dx.doi.org/10.1016/j.carbpol.2014.11.004
0144-8617/

spectral complications that arise from intra- and intermolecular hydrogen bonds between unsubstituted hydroxyl groups of CA. From the ring carbons in the ^{13}C NMR spectra of CA, acetylation of the hydroxyl group at the 6-position is confirmed by the deshielding of C6, while the C2 and C3 resonances of the AGU overlap the C5 resonance, and therefore do not allow direct observation of the impact of acetyl substitution at the 2- and 3-positions (Goodlett, Dougherty, & Patton, 1971). Instead, acetyl substitution at the 2- and 3-positions of cellulose is thought to result in the shielding of C1 and C4, respectively (Miyamoto, Sato, Shibata, Inagaki, & Tanahashi, 1984), although this has not been directly confirmed by NMR. Therefore, there are still uncertainties about the NMR spectra of CA.

In order to correlate the structure and properties of CA, the chemical shift assignments must be known in detail. In addition, a direct observation of the chemical shift changes that occur with acetyl substitution of cellulose provides useful information about the conformational properties and the molecular dynamics (Kamide & Okajima, 1981). From these points of view, an unambiguous chemical shift assignment for the protons and carbons is required to understand the CA structure. However, the assignment of ring protons and carbons is difficult, with the exception of cellulose triacetate, because the eight AGUs, i.e., 2,3,6-tri-, 2,3-di-, 2,6-di-, 3,6-di-, 2-mono-, 3-mono-, 6-mono-, and unacetylated AGUs, overlap each other in both the ^{1}H and ^{13}C NMR spectra of CA. Moreover, Hikichi, Kakuta, and Katoh (1995) detected nine different ^{1}H—^{1}H spin networks for AGUs in COSY and relayed COSY spectra of CA (DS = 2.46), and suggested that the nine AGUs are due to four different 2,3,6-triacetylated AGUs, two 2,3-diacetylated AGUs, one 2,6-diacetylated AGU, one 3,6-diacetylated AGU, and one 6-monoacetylated AGU based on the ^{1}H chemical shifts (Hikichi et al., 1995). The authors believe that the variation of the ^{1}H—^{1}H spin networks arising from the same AGU is due to different neighbors on either side of the AGU. If this hypothesis is correct, then there are 64 different species possible for each AGU because each AGU can be flanked by any of the seven acetylated AGUs or the unacetylated AGU. Therefore, precise chemical assignment of the AGUs comprising of CA, as well as direct observation of the chemical shift changes accompanying acetylation, still remain a great challenge in the cellulose chemistry.

Recently, the authors reported the two-dimensional NMR characterization of CA with a DS of 2.33, in order to determine the chemical shift assignment of a monomer comprising CA (Kono, 2013a). However, the structural characterization of CAs with a wide DS range is required in order to obtain detailed structural information of CA such as the chemical shift change accompanying a DS change. In this study, CA samples with DS ranging from 2.92 to 0.92 were prepared by the acid-hydrolysis of CA with a DS of 2.92. The precise ^{1}H and ^{13}C chemical shift assignments of the AGUs containing CA were determined by measuring the COSY, TOCSY, and HSQC spectra of the CA samples dissolved in DMSO-d_6 and cellulose powder dissolved in TBAF/DMSO-d_6. DMSO is usually used as an NMR solvent for the characterization of CA in many reports (Qu, Kishimoto, Kishino, Hamada, & Nakajima, 2011; Qu, Kishimoto, Ogita, Hamada, & Nakajima, 2012; Kim & Ralph, 2010; Kim & Ralph, 2014). The TBAF/DMSO solvent system is a powerful solvent that is frequently used for the dissolution of cellulose or wood, and is applied for the homogeneous acetylation of cellulose (Heinze et al., 2000; Heinze, 1998; Köhler & Heinze, 2007; Ass, Frollini, & Heinze, 2004; Lu, & Ralph, 2003). On the basis of the ^{1}H and ^{13}C chemical shift data for each AGU, the substituent effect of the acetyl groups at the 2-, 3-, and 6-positions on the ^{1}H and ^{13}C chemical shifts of each ring proton and carbon were determined. Moreover, the chemical shift additivity observed for CA is discussed with respect to the substituent effects using the chemical shift data obtained in this study.

2. Experimental

2.1. Materials

CA **1** (DS of 2.92 and average molecular weight of 1.8×10^5) and fibrous cellulose powder CF-11 were purchased from Sigma-Aldrich Co. (USA) and Whatman International Ltd. (UK), respectively. All the other chemicals, which were purchased from Kanto Chemicals (Japan) and Wako Pure Chemicals (Japan), were of reagent grade and were used as received.

2.2. Preparation of CA samples

Typically, 1.0 g of CA **1** was dissolved in 20 mL of acetic acid. Concentrated sulfuric acid (0.40 g) was added to the solution followed by water (2.2 mL). The mixture was allowed to react at 358 K for 15, 45, and 80 min to obtain CA **2**–**4**, respectively. At the end of the reaction, a 20% aqueous magnesium acetate solution was added to neutralize the sulfuric acid. The product was precipitated and washed in ethanol. The precipitates were suspended in water, dialyzed using dialysis tubing (Mw 12000 cut-off, Thermo Fisher Scientific Inc., USA) for 3–7 days until completely neutralized, and then freeze-dried. All the samples were stored in a desiccator under vacuum until the time of use.

2.3. Perpropionylation of CA samples

Perpropionylations of CA **1**–**4** were performed according to the previously reported method (Tezuka & Tsuchiya, 1995). Each CA (0.25 g) dissolved in 6 mL of pyridine was allowed to react with 6 mL of propionic anhydride in the presence of 0.1 g of DMAP as a catalyst for 24 h at 358 K. The perpropionylated CA was precipitated and washed with ethanol (100 mL) three times. The sample was reprecipitated from 3 mL of chloroform in 100 mL of ethanol, then filtered and dried at 358 K under vacuum.

2.4. NMR spectroscopy

All the NMR experiments were performed on a Bruker AVIII 500 spectrometer operating at 500.13 MHz for ^{1}H experiments and 125.13 MHz for ^{13}C experiments, and equipped with a 5 mm dual-resonance BBO probe incorporating gradients for the *z*-axis (Bruker BioSpin GmbH, Germany). All the spectra were acquired and processed with Bruker TopSpin version 3.0 on a Windows PC. CA samples (10–20 mg) were dissolved in 600 μL of DMSO-d_6, cellulose samples were dissolved in 600 μL of 5% (w/v) TBAF/DMSO-d_6, and the perpropionylated CA samples (20 mg) were dissolved in 600 μL of $CDCl_3$. Each solution was placed in a 5 mm NMR glass tube (Wilmad-Labglass Co., USA). The sample temperatures were set to 313 K for the samples in $CDCl_3$ and to 363 K for the samples in DMSO-d_6 and TBAF/DMSO-d_6. 1D ^{1}H, 1D ^{13}C, ^{1}H inverse-gated decoupled 1D ^{13}C (Zhou et al., 2007), 2D ^{1}H—^{1}H COSY using a gradient pulse for selection (Trimbre & Bernstein, 1994), 2D ^{1}H—^{1}H TOCSY using the MLEV17 sequence (Bax & Davis, 1985; Braunschweiler & Ernst, 1983) for TOCSY spin-locking, and 2D ^{1}H—^{13}C HSQC via INEPT transfer (Bax, Griffey, & Hawkins, 1983; Bax & Subramanian, 1986) using Echo/Antiecho-TPPI gradient selection (Kay, Keifer, & Saarinen, 1992) with ^{1}H decoupling during acquisition using trim pulses (Bax & Davis, 1985; Braunschweiler & Ernst, 1983) in INEPT transfer were performed for the CA and cellulose samples. 1D ^{1}H, 1D ^{13}C, and ^{1}H inverse-gated decoupled 1D ^{13}C experiments were also performed for the perpropionylated CA samples. In the COSY experiments, a total of 256 t_1 acquisitions with 128 scans per increment were collected. In the TOCSY experiments, the mixing times were 200 ms, and a total of 256 t_1 acquisitions with 128 scans per increment were collected. In the

HSQC experiments, the delay time was 3.44 ms, which corresponds to a J_{C-H} of 145 Hz, and a total of 196 t_1 acquisitions with 512 scans per increment were collected. The repetition time was set to 45 s for the ^{1}H inverse-gated decoupled 1D ^{13}C experiments and to 2 s for all other NMR experiments. The ^{1}H and ^{13}C chemical shifts of the NMR data were calibrated by assigning the solvent residual peak of $CHCl_3$ as 7.26 ppm for ^{1}H and 77.36 ppm for ^{13}C and that of DMSO as 2.50 ppm for ^{1}H and 39.52 ppm for ^{13}C.

3. Results and discussion

3.1. ^{1}H and ^{13}C NMR spectra of CAs

Fig. 1 shows the quantitative ^{13}C NMR spectra of CA samples **1**–**4** recorded using the inverse-gated ^{1}H decoupling method. The integral values for each ^{13}C resonance when that of C1 is set to 1 are shown in the spectra. The DS of these CA samples equals the integral value of the carbonyl carbons. The DS values of CA **1**–**4** are 2.92, 2.12, 1.66, and 0.92, respectively. As described in previous reports (Goodlett et al., 1971), the intensities of the C1 resonances at 98 and 102 ppm and that of the C6 resonances at 62 and 58 ppm depend on the DS of CA. C1 at 98 ppm and C6 at 62 ppm increase when the DS values increase, whereas C1 at 102 ppm and C6 at 58 ppm decrease with the increase in DS values. The C2–C5 resonances of the CAs,

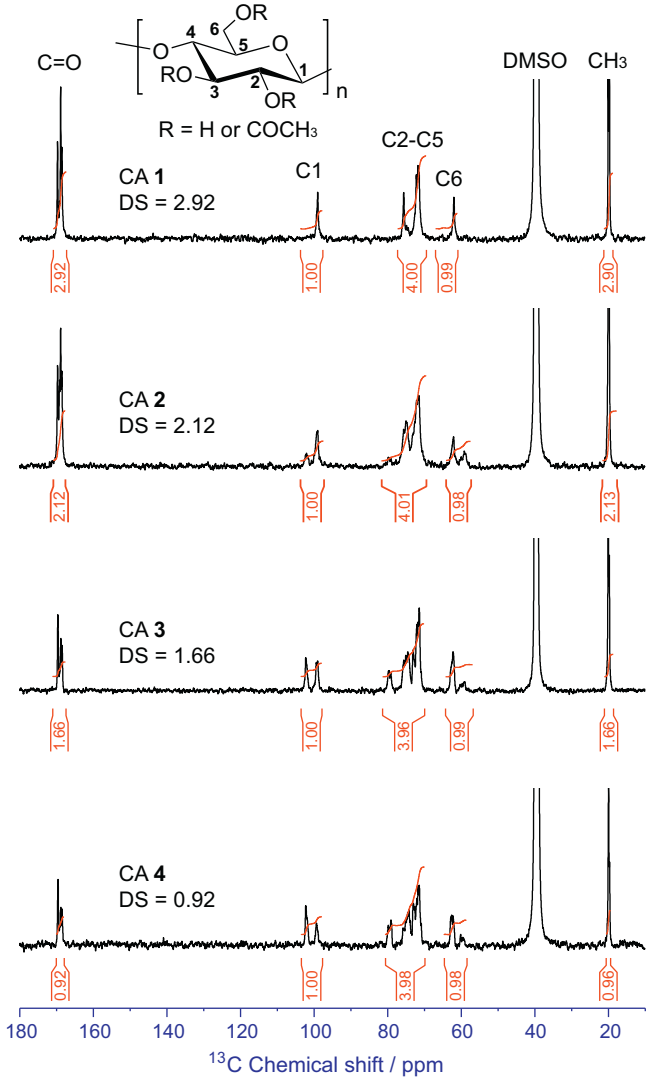

Fig. 1. Quantitative ^{13}C NMR spectra of CA **1**–**4** in DMSO-d_6 recorded at 363 K.

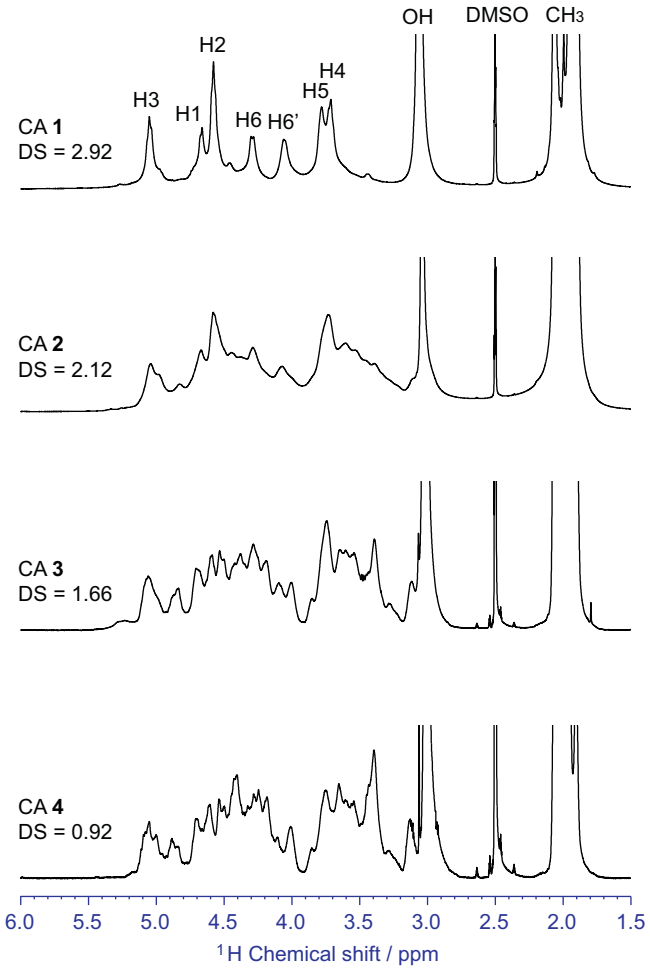

Fig. 2. ^{1}H NMR spectra of CA **1**–**4** in DMSO-d_6 recorded at 363 K.

with the exception of CA **1**, exhibit very complicated spectral lines in the 85–70 ppm region because the ^{13}C resonances of the various AGUs with different substituent distributions are overlapped. The ^{1}H NMR spectra of CA **2**–**4**, as shown in Fig. 2, also exhibit very complicated spectral lines in the ring proton region (5.3–2.8 ppm), whereas the spectra of CA **1** shows seven clearly resolved proton resonances, owing to its 2,3,6-triacetylated AGUs.

3.2. Individual DS of CAs

As shown in Fig. 3, the individual DS at the 2-, 3-, and 6-positions of CA **1**–**4** were determined from the quantitative ^{13}C NMR spectra of the perpropionylated derivatives of the CA samples. The acetyl carbonyl triplet (170.5–169 ppm) is observed at a position distinctly separated from that of the propionyl carbonyl triplet (173.5–172 ppm). The resonances at 170.1, 169.6, and 169.2 ppm can be assigned to the acetyl carbonyl carbons at the 6-, 3-, and 2-positions, respectively, and the resonances at 173.6, 173.2, and 172.7 ppm are assigned to the propionyl carbonyl carbons at the 6-, 3-, and 2-positions, respectively (Tezuka & Tsuchiya, 1995). The quantitative evaluation of the acetyl triplet resonances permits the determination of the individual DS values at the 2-, 3-, and 6-positions of the AGUs (Table 1). The acetyl substituent distribution of the CAs is ranked as follows: 6 > 2 = 3. This result is in agreement with previously reported results on the substituent distribution of a series of CAs prepared from cellulose triacetate by the acid-hydrolysis treatment (Miyamoto et al., 1984).

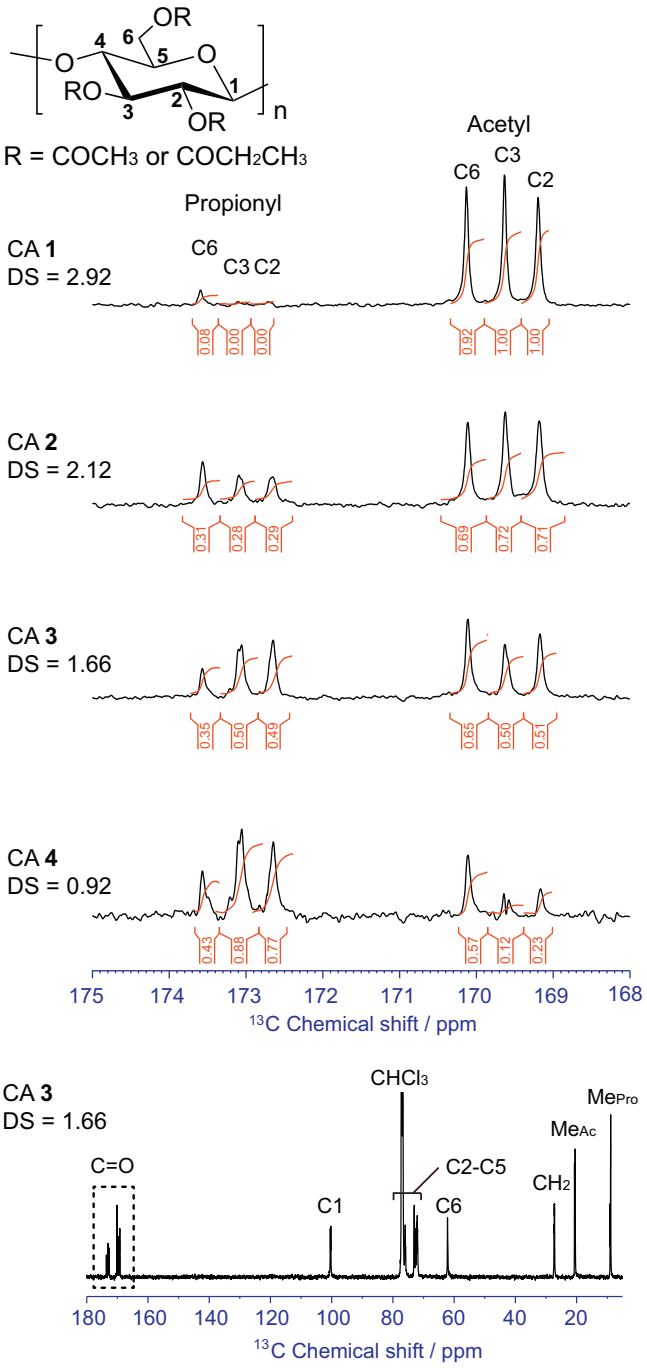

Fig. 3. Expansion of the carbonyl carbon region (175–168 ppm) of the quantitative ^{13}C NMR spectra of perpropionylated CA **1**–**4** in $CDCl_3$ recorded at 313 K. The full spectrum of CA **3** is shown at the bottom of this figure. The integral values for the carbonyl carbons of each CA are normalized so that the sum of the integral values of the carbonyl carbons is equal to the DS.

3.3. ^{1}H—^{1}H and ^{1}H—^{13}C correlation spectra of CAs and cellulose

Fig. 4 shows the contour plots of the COSY, TOCSY, and HSQC spectra of CA **1**. The COSY spectrum provides the directly coupled ^{1}H—^{1}H spin couplings of CA, and the TOCSY spectrum recorded with a spin-lock time of 200 ms, which provides the long-range ^{1}H—^{1}H spin couplings, is stacked on the COSY spectrum. The two sets of ^{1}H—^{1}H spin correlation networks comprised of the seven protons (H1 to H6′) of the AGU detected in the TOCSY spectrum, along with the vicinal ^{1}H—^{1}H couplings of each ^{1}H resonance in the COSY spectrum, allowed the complete assignment of the ^{1}H resonances for the ring protons. Since the individual DS at the 2-, 3-, and 6-positions of CA **1** are 1, 1, and 0.92, respectively, the main correlation network connected by black lines is assigned to the 2,3,6-triacetylated AGU, and the minor network connected by red lines is assigned to the 2,3-diacetylated AGU. The HSQC spectrum of CA **1**, which provides the directly coupled ^{1}H—^{13}C spin coupling, allowed assignment of the ^{13}C chemical shifts for the ring carbons in the two AGUs.

In the COSY and TOCSY spectra of CA **2** (DS = 2.12, Fig. 5), the spin correlation networks due to the 2,3,6-triacetylated and 2,3-diacetylated AGUs detected in the spectra of CA **1** (DS = 2.92) were observed. The ^{1}H and ^{13}C chemical shifts of these AGUs in CA **2** completely agreed with those in CA **1**, indicating that the effect of neighboring AGUs in the cellulose chain on the ^{1}H and ^{13}C chemical shifts of the AGU is negligible. In addition to these correlations, two additional sets of ^{1}H—^{1}H correlation networks comprising seven protons were detected, as depicted by the blue and green lines in the spectra. A distinctive feature of the ^{1}H—^{1}H correlation network connected by blue lines is the chemical shift of H3 (3.4 ppm),

Table 1
DS and individual DS at position *i* (=2, 3, or 6) of CA **1**–**4**.

Sample	DS[a]	Individual DS_i[b]			Individual DS_i'[c]		
		i = 2	*i* = 3	*i* = 6	*i* = 2	*i* = 3	*i* = 6
CA **1**	2.92	1.00	1.00	0.92	1.00	1.00	0.91
CA **2**	2.12	0.71	0.72	0.69	0.73	0.72	0.66
CA **3**	1.66	0.51	0.50	0.65	0.52	0.52	0.65
CA **4**	0.92	0.23	0.12	0.57	0.27	0.13	0.61

[a] DS was determined from the integral values of the carbonyl carbons in the quantitative ^{13}C NMR spectra of each CA (Fig. 1).
[b] Individual DS_i (*i* = 2, 3, or 6) were determined from the integral values of each acetyl carbon in the quantitative ^{13}C NMR spectra of the perpropionylated derivative of each CA (Fig. 3).
[c] Individual DS_i' (*i* = 2, 3, or 6) were determined from the quantitative ^{13}C NMR spectra of each CA (Fig. 8). DS_2' and DS_6' are the integral values of the C1 and C6 resonances, respectively, and DS_3' was determined using the following equation: $DS_3' = 1 -$ (Integral value of C4′).

Table 2
^{1}H and ^{13}C chemical shifts (δ) of the AGUs comprising CA in DMSO-d_6 and cellulose in TBAF/DMSO-d_6 at 363 K.

Substituted positions	δ[a] (ppm)						
	H1	H2	H3	H4	H5	H6	H6′
2,3,6	4.67	**4.58**	**5.07**	3.72	3.75	**4.28**	**4.07**
2,3	4.62	**4.55**	**4.96**	3.78	3.41	3.76	3.62
2,6	4.76	**4.68**	3.51	3.52	3.73	**4.20**	**4.03**
3,6	4.35	3.12	**4.83**	3.58	3.64	**4.38**	**4.07**
2	4.70	**4.62**	3.48	3.53	3.44	3.67	3.58
3	4.48	3.27	**4.95**	3.62	3.40	3.82	3.62
6	4.36	2.98	3.40	3.39	3.76	**4.29**	**4.00**
Unsubstituted (Cellulose)	4.42	3.13	3.43	3.41	3.46	3.74	3.65
	4.40	3.11	3.41	3.41	3.36	3.73	3.65

	δ[a] (ppm)					
	C1	C2	C3	C4	C5	C6
2,3,6	98.8	**71.3**	**72.0**	75.7	71.7	**61.8**
2,3	98.8	**71.2**	**72.4**	74.4	74.7	58.5
2,6	99.0	**72.9**	71.6	79.6	71.6	**62.3**
3,6	101.9	71.2	**74.2**	75.9	71.6	**61.9**
2	98.9	**73.0**	71.6	79.1	75.1	59.9
3	101.6	70.7	**74.1**	74.8	74.1	58.8
6	102.4	73.2	73.9	79.2	71.4	**62.9**
Unsubstituted (Cellulose)	102.0	72.9	73.9	79.1	74.3	60.1
	102.1	72.9	74.0	78.9	74.8	60.1

[a] The δ values were determined from the 2D contour plots of the TOCSY and HSQC spectra of CA **1**, **2**, and **4**, and cellulose, as shown in Figs. 4–7. The δ values shown in bold are the substituted positions.

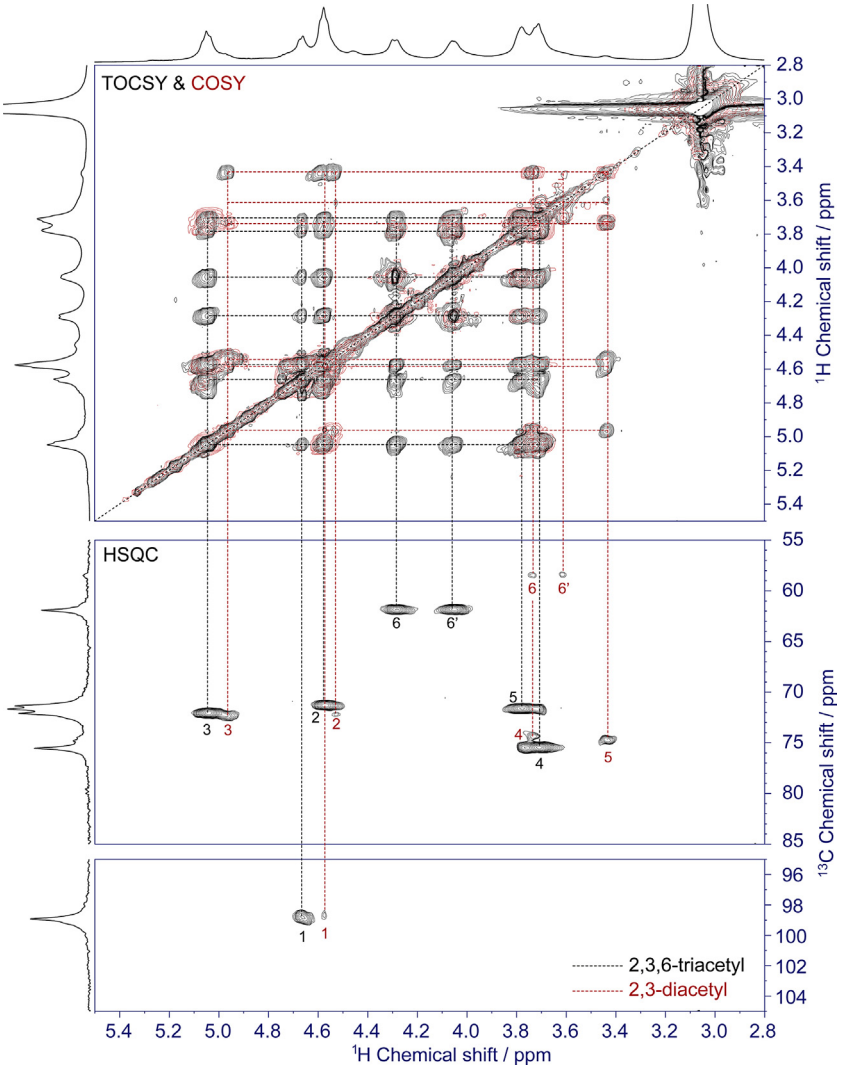

Fig. 4. 2D contour plots of the COSY (top; red lines), TOCSY (top; black lines), and HSQC (bottom; black lines) spectra of CA **1** (DS = 2.92) in DMSO-d_6 recorded at 363 K. The through-bond ^{1}H—^{1}H and ^{1}H—^{13}C spin couplings of the 2,3,6-triacetylated and 2,3-diacetylated AGUs are shown by the dotted black and red lines in these spectra, respectively. (For interpretation of the references to color in this figure legend, the reader is referred to the web version of this article.)

which is considerably shifted upfield in comparison with the H3 chemical shift of the 2,3,6-triacetylated AGU (5.1 ppm). Similarly, a notable feature of the ^{1}H—^{1}H correlation network connected by green lines is the chemical shift of H2 (3.1 ppm), which is considerably shifted upfield in comparison with the H2 chemical shift of the 2,3,6-triacetylated AGU (4.6 ppm). These features allowed the ^{1}H—^{1}H correlation networks connected by the blue and green lines to be assigned to the 2,6- and 3,6-diacetylated AGUs, respectively. The HSQC spectra allowed precise assignment of the ^{13}C resonances of these AGUs.

In the case of CA **4** (DS = 0.92, Fig. 6), the TOCSY spectra was dominated by four new sets of ^{1}H—^{1}H spin correlation networks connected by red, blue, green, and black lines. The DS of CA **4** is 0.92, and thus, three of the ^{1}H—^{1}H spin networks are due to monoacetylated AGUs. In comparison with the ^{1}H chemicals shifts of the 2,3,6-triacetylated AGU, the H3 and H6 chemical shifts of the AGU connected by red lines, the H2 and H6 chemical shifts of the AGU connected by blue lines, and the H2 and H3 chemical shifts of the AGU connected by green lines are all shifted upfield, indicating that the AGUs connected by red, blue, and green lines could be assigned to the 2-, 3-, and 6-monoacetylated AGUs, respectively. The remaining ^{1}H—^{1}H correlation network connected by black lines is assigned to the unacetylated AGU, because the chemical shifts of H2, H3, H6, and H6′ of this AGU are shifted upfield by 1.64–0.50 ppm in comparison with those of the 2,3,6-triacetylated AGU. The HSQC spectra of CA **4** provided the ^{13}C chemical shifts of the three mono-acetylated AGUs and the unacetylated AGU. To confirm the chemical shift assignments for the unacetylated AGU, comparable 2D spectra of cellulose dissolved in TBAF/DMSO-d_6 were measured (Fig. 7). The ^{1}H and ^{13}C chemical shifts of cellulose are almost the same as those of the unacetylated AGU detected in the CA **4** spectra, although there are slight differences in the chemical shifts between these AGUs (~0.13 ppm for ^{1}H and ~0.5 ppm for ^{13}C). This result indicated that the assignment of the unacetylated AGU is accurate. The ^{1}H and ^{13}C resonance assignments for the eight AGUs containing CA are summarized in Table 2.

The results of the chemical shift assignments proved the previous interpretation of the ^{13}C resonance splitting in the C1, C4, and C6 regions (Goodlett et al., 1971; Miyamoto et al., 1984). The chemical shifts of C1 when the neighboring C2 is substituted with an acetyl group shifted from 102 ppm to 99.0–98.8 ppm, those of C4 when the neighboring C3 is substituted shifted from 79.1 ppm to 75.9–74.4 ppm, and the substituted C6 was deshielded and shifted from 60.1 ppm to 61.6–62.9 ppm. The integral values for these C1, C4, and C6 regions, as well as the other carbon regions of the

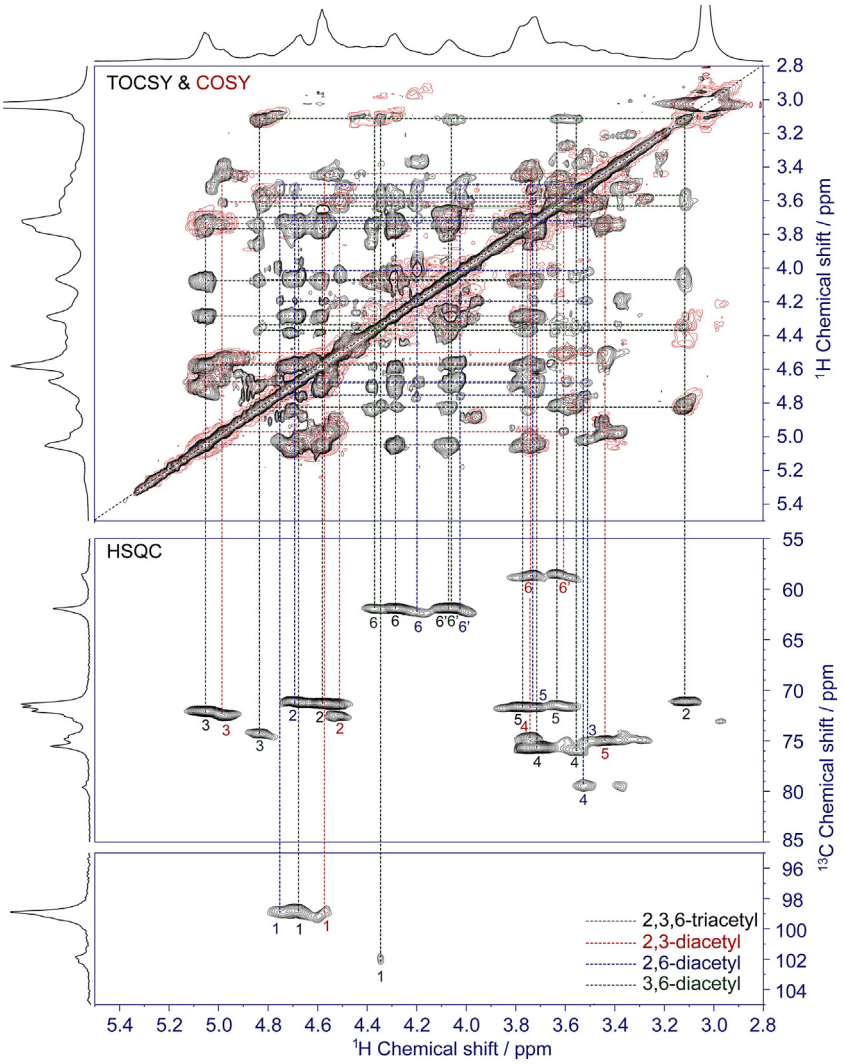

Fig. 5. 2D contour plots of the COSY (top; red lines), TOCSY (top; black lines), and HSQC (bottom; black lines) spectra of CA **2** (DS = 2.12) in DMSO-d_6 recorded at 363 K. The through-bond ^{1}H—^{1}H and ^{1}H—^{13}C spin couplings of the 2,3,6-triacetylated and 2,3-, 2,6-, and 3,6-diacetylated AGUs are shown by the dotted black, red, blue, and green lines in these spectra, respectively. (For interpretation of the references to color in this figure legend, the reader is referred to the web version of this article.)

CA samples, are shown in Fig. 8. The individual DS at the 2-, 3-, and 6-positions determined from the integral values of the C1, C4, and C6 regions are shown in Table 1 (individual DS_i' (i = 2, 3, and 6)). These values are in complete agreement with the individual DS values determined from the analysis of the perpropionylated derivatives (Table 1 and Fig. 3). This result indicates that the individual DS of a CA can be precisely determined by the analysis of these ring carbon regions without derivatization of the CA, although a longer measurement time is required to obtain the ^{13}C spectra of CAs than to obtain those of the perpropionylated CA derivatives.

3.4. Acetyl group substituent effects

The effect of substitution at the 2-, 3-, or 6-positions on the chemical shift of each AGU was estimated from the chemical shift difference ($\Delta\delta_i$, i = 2, 3, or 6) between the monoacetylated AGUs and the unacetylated AGU at each position. Each $\Delta\delta_i$ value was calculated using the following equations (Eqs. (1)–(3)):

$$\Delta\delta_{i=2} = \delta(2 - \text{monoacetylated AGU}) - \delta(\text{unacetylated AGU}) \quad (1)$$

$$\Delta\delta_{i=3} = \delta(3 - \text{monoacetylated AGU}) - \delta(\text{unacetylated AGU}) \quad (2)$$

$$\Delta\delta_{i=6} = \delta(6 - \text{monoacetylated AGU}) - \delta(\text{unacetylated AGU}) \quad (3)$$

where the δ values are the ^{1}H and ^{13}C chemical shifts of each AGU. The $\Delta\delta_i$ values determined by applying the chemical shift data of the monoacetylated AGUs and the unacetylated AGU (Table 2) to Eqs. (1)–(3) are summarized in Table 3. A comparative analysis of the $\Delta\delta_i$ values indicated that acetyl substitution at the 2-, 3-, and 6-positions resulted in a large upfield shift of the adjacent carbons (γ-effect, i.e., through three bonds from the substituent). Substitution at the 2-position led to a 3.1 and 2.3 ppm upfield shift for C1 and C3, respectively, substitution at the 3-position caused a 2.2 and 4.3 ppm upfield shift for C2 and C4, respectively, and substitution at the 6-position caused a 2.9 ppm upfield shift for C5. Similar γ-effects were also observed for the ^{1}H $\Delta\delta_i$ values; substitution at the 2- and 3-positions caused a ca. 1.5 ppm downfield shift for both H2 and H3, and substitution at the 6-position caused a 0.55–0.42 ppm downfield shift for H6 and H6′. In addition, substitution at the 6-position caused a significant change in the chemical shift of the directly attached carbon (β-effect, i.e. through two bonds from the substituent); the C6 chemical shift was shifted 2.8 ppm downfield by substitution at position 6. Conversely, the β-effects from substitution at the 2- and 3-positions

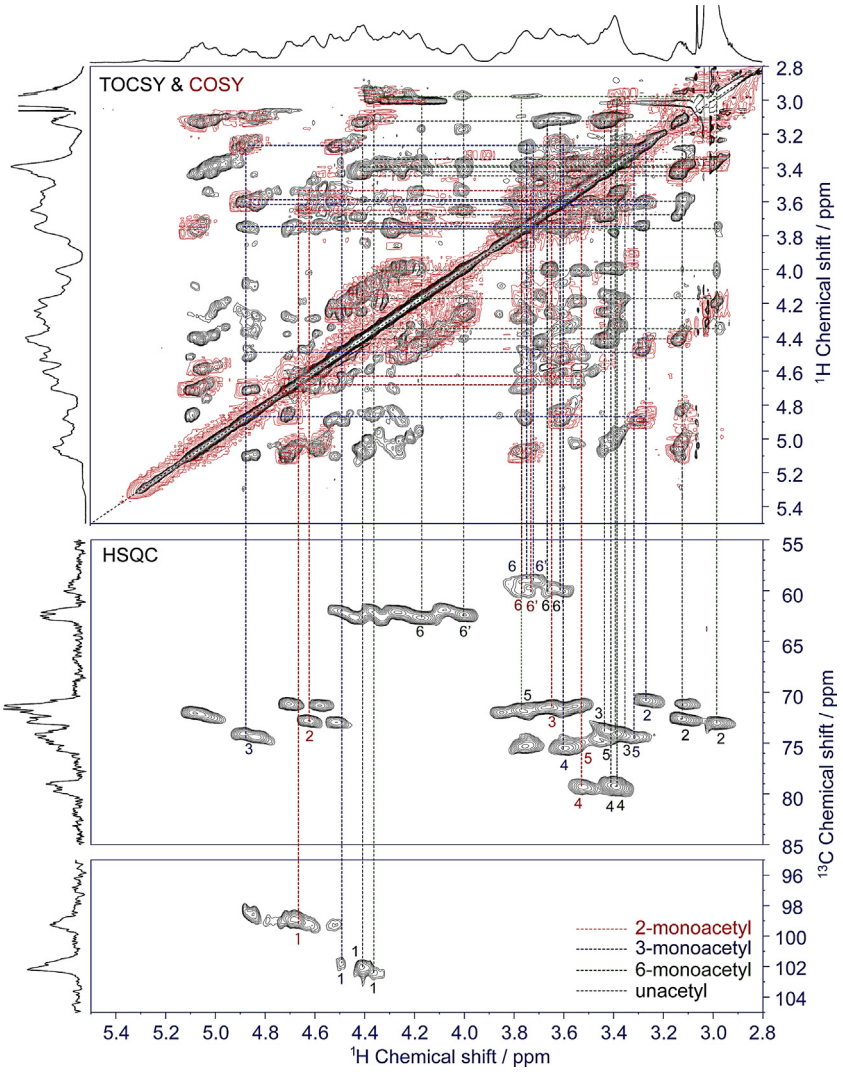

Fig. 6. 2D contour plots of the COSY (top; red lines), TOCSY (top; black lines), and HSQC (bottom; black lines) spectra of CA **4** (DS = 0.92) in DMSO-d_6 recorded at 363 K. The through-bond ^{1}H—^{1}H and ^{1}H—^{13}C spin couplings of the 2-, 3-, and 6-monoacetylated and the unacetylated AGUs are shown by the dotted red, blue, green, and black lines in these spectra, respectively. The through-bond ^{1}H—^{1}H and ^{1}H—^{13}C spin couplings of the 2,3,6-triacetylated and 2,3-, 2,6- and 3,6-diacetylated AGUs agreed with those shown in Fig. 5 and are omitted from this figure. (For interpretation of the references to color in this figure legend, the reader is referred to the web version of this article.)

were very small; substitution at positions 2 and 3 caused only a 0.1 ppm and 0.2 ppm downfield shift for the directly attached C2 and C3, respectively. δ-effects arising through four bonds from the acetyl substituents were very small or negligible at each position in both the ^{1}H and ^{13}C spectra. From these findings, the most notable difference between the substituent effects at the 2- and 3-positions and that at position 6 was the β-effect. Although the reason for this difference is not clear, it is related to the conformation of the acetyl groups; the acetyl groups substituted at the 2- and 3- positions are attached to the rigid hexose ring, whereas the acetyl group at the 6-position has conformational flexibility around the C5—C6 bond to form the most stable conformation, i.e. *gauche–gauche* for the O6—C6—C5—O5 torsion angle (Kono, 2013b, 2004; Kono, Erata, & Takai, 2002; Kono, Erata, & Takai, 2003; Kono, Numata, Erata, & Takai, 2004).

Table 3
Substituent effects ($\Delta\delta_i$, i = 2, 3,and 6) on the δ of CAs by substitution at the 2-, 3-, or 6-positions.

Substituted positions	$\Delta\delta_i$[a]/ppm						
	H1	H2	H3	H4	H5	H6	H6′
i = 2	0.28	**1.49**	0.05	0.12	−0.02	−0.07	0
i = 3	0.06	0.14	**1.52**	0.21	−0.06	0.08	0.04
i = 6	−0.06	−0.15	−0.15	−0.02	0.30	**0.55**	**0.42**

	$\Delta\delta_i$[a] (ppm)					
	C1	C2	C3	C4	C5	C6
i = 2	−3.1	**0**	−2.3	0.3	0.8	−0.2
i = 3	−0.4	−2.2	**0.2**	−4.3	−0.2	−1.3
i = 6	0.4	0.3	0	0.1	−2.9	**2.8**

[a] $\Delta\delta_i$ were determined by applying the ^{1}H and ^{13}C chemical shifts of the 2-, 3-, and 6-monoacetylated AGUs and unacetylated AGU (as summarized in Table 2) to Eqs. (1)–(3) in the text.

3.5. Chemical shift additivity by acetyl substitution

Generally, NMR chemical shifts have additivity and the effects of substitution on the ^{1}H and ^{13}C NMR chemical shifts of various compounds have been investigated. This additivity has frequently been applied for the prediction of chemical shifts, estimation of chemical shifts for new compounds, and conformational analysis (Allred & Rochow, 1957; Dailey & Shoolery, 1955; Paul & Grant, 1963; Zürcher, 1967). Therefore, it is important to evaluate whether chemical shift additivity could be applied to acetyl

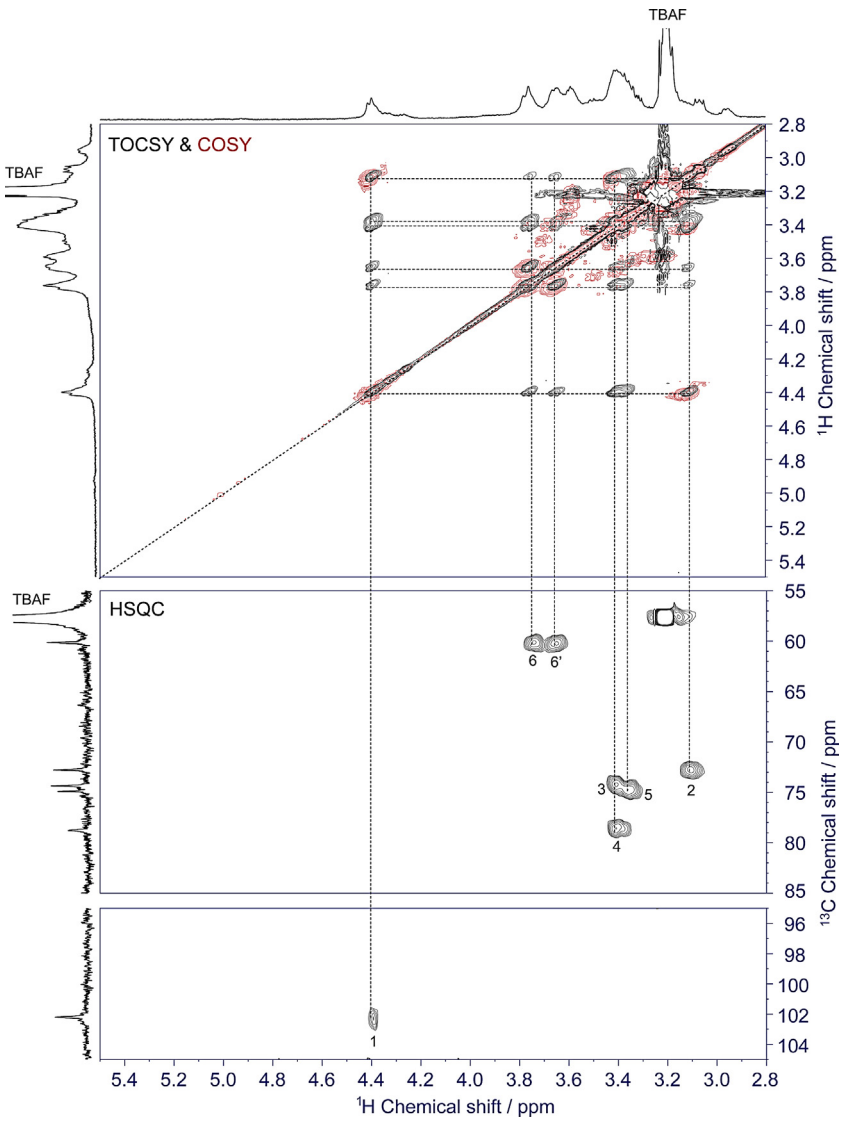

Fig. 7. 2D contour plots of the COSY (top; red lines), TOCSY (top; black lines), and HSQC (bottom; black lines) spectra of cellulose in TBAF/DMSO-d_6 recorded at 363 K. The through-bond ^{1}H—^{1}H and ^{1}H—^{13}C spin couplings of the AGU are shown by the dotted black lines in these spectra. (For interpretation of the references to color in this figure legend, the reader is referred to the web version of this article.)

substitution in cellulose. If chemical shift additivity is applicable to the chemical shifts of the AGUs in CA, the chemical shifts of the 2,3-, 2,6-, and 3,6-diacetylated and 2,3,6-triacetylated AGUs (δ_{cal}) could be calculated using the following equations (Eqs. (4)–(7)):

$$\delta_{cal}(2,3-\text{diacetylated AGU}) = \delta(\text{unacetylated AGU}) + \Delta\delta_{i=2} + \Delta\delta_{i=3} \quad (4)$$

$$\delta_{cal}(2,6-\text{diacetylated AGU}) = \delta(\text{unacetylated AGU}) + \Delta\delta_{i=2} + \Delta\delta_{i=6} \quad (5)$$

$$\delta_{cal}(3,6-\text{diacetylated AGU}) = \delta(\text{unacetylated AGU}) + \Delta\delta_{i=3} + \Delta\delta_{i=6} \quad (6)$$

$$\delta_{cal}(2,3,6-\text{triacetylated AGU}) = \delta(\text{unacetylated AGU}) + \Delta\delta_{i=2} + \Delta\delta_{i=3} + \Delta\delta_{i=6} \quad (7)$$

where δ (unacetylated AGU) is the chemical shift of the unacetylated AGU, and $\Delta\delta_i$ (i = 2, 3, or 6) is the difference in chemical shifts between the unacetylated AGU and the mono-acetylated AGUs (Table 3). The chemical shifts calculated for the 2,3-, 2,6-, and 3,6-diacetylated and 2,3,6-triacetylated AGUs are summarized in Table 4. The calculated chemical shift data for these four AGUs are almost equal to the experimental data (Table 2), and the differences are <0.21 ppm for ^{1}H and <1.0 ppm for ^{13}C chemical shifts. This finding indicates that the chemical shift additivity could be applied to CA and that the changes in the ^{1}H and ^{13}C chemical shifts observed in the acetylated AGUs containing CA are almost completely explained by the substituent effects of the acetyl groups in the 2-, 3-, and 6-positions, including β-, γ-, and δ-effects. The slight differences between the experimentally determined chemical shifts and the calculated chemical shifts are likely due to hydrophobic interactions between the AGUs and the solvent, hydrogen bond formation between unsubstituted hydroxyl groups, etc., although the relationship between these interactions and the changes in the chemical shifts are not clear.

In this study, we have provided chemical shift data for the AGUs containing CA, by using CA samples with a wide range of

Table 4
The calculated ^{1}H and ^{13}C chemical shifts (δ_{cal}) of 2,3-, 2,6-, and 3,6-diacetylated AGUs and 2,3,6-tricacetylated AGU and the difference between the calculated and experimentally determined chemical shifts.

Substituted positions	δ_{cal}[a]/ppm						
	H1	H2	H3	H4	H5	H6	H6′
2,3,6	4.70 (−0.03)	4.61 (−0.03)	4.97 (0.10)	3.72 (0)	3.68 (0.07)	4.30 (−0.02)	4.04 (0.03)
2,3	4.76 (−0.14)	4.76 (−0.21)	5.00 (−0.04)	3.74 (0.04)	3.38 (0.03)	3.75 (0.01)	3.62 (0)
2,6	4.64 (0.12)	4.47 (0.21)	3.45 (0.06)	3.51 (0.01)	3.74 (−0.01)	4.22 (−0.02)	4.00 (0.03)
3,6	4.42 (−0.07)	3.12 (0)	4.92 (−0.09)	3.60 (−0.02)	3.70 (−0.06)	4.37 (0.01)	4.04 (0.03)
	δ_{cal}[a] (ppm)						
	C1	C2	C3	C4	C5	C6	
2,3,6	98.9 (−0.1)	71.1 (0.2)	71.8 (0.2)	75.2 (−0.5)	72 (−0.3)	61.4 (0.4)	
2,3	98.5 (0)	70.8 (0.3)	71.8 (0.4)	75.1 (−0.7)	74.9 (−0.2)	58.6 (−0.1)	
2,6	99.3 (−0.3)	73.3 (−0.4)	71.6 (0)	79.5 (0.1)	72.2 (−0.6)	62.7 (−0.4)	
3,6	102.0 (−0.1)	71.0 (0.2)	74.1 (0.1)	75.1 (1.0)	71.2 (0.4)	61.6 (0.3)	

[a] δ_{cal} were determined by applying each $\Delta\delta_i$ value (Table 3) and the δ value of the unacetylated AGU (Table 2) to Eqs. (4)–(7) in the text. The numbers in parentheses indicate the chemical shift difference between the experimentally determined chemical shift (δ) and the calculated chemical shift (δ_{cal}).

DS. It was revealed that the chemical shift change of each AGU was independent of the DS. Thus, the chemical shift data could be useful for characterizing the CA structure. For example, the monomers as well as individual DS of CA samples dissolved in DMSO can be quantitatively estimated by NMR, without any pretreatment.

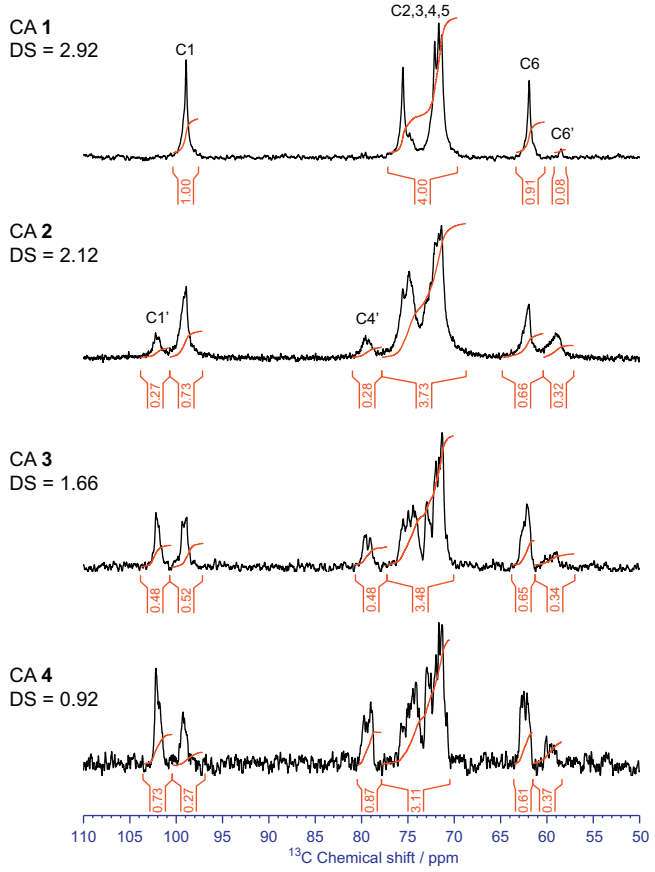

Fig. 8. The ring carbon region (110–60 ppm) of the quantitative ^{13}C NMR spectra of CA **1**–**4** in DMSO-d_6 recorded at 363 K (partial expanded region of Fig. 1). C1′, C4′, and C6′ are the resonances of C1 when the neighboring position 2 is unsubstituted, C4 when the neighboring position 3 is unsubstituted, and unsubstituted C6, respectively.

4. Conclusion

A comparative analysis of the ^{1}H and ^{13}C chemical shift data for the AGUs containing CA revealed the effects of substitution by acetyl groups at the 2-, 3-, and 6-positions. In addition, chemical shift additivity of the acetyl substituent effects was confirmed and can be applied to the ^{1}H and ^{13}C nuclei containing the AGUs in CA. These substituent effects will be applied to the conformational analysis of CA at the molecular level. In addition, further exploration of substituent effects for other functional groups will be useful for the characterization of other complicated cellulose derivatives.

Acknowledgements

This work was supported in part by Grants-in-Aid for Scientific Research C-25410134 from the Japan Society for Promotion of Science (JSPS).

References

Allred, A. L., & Rochow, E. G. (1957). The nuclear magnetic resonance absorption of hydrogen in methyl groups. The electronegativity of substituents. *Journal of the American Chemical Society*, *79*, 5361–5365.
Ass, B. A. P., Frollini, E., & Heinze, T. (2004). Studies on the homogeneous acetylation of cellulose in the novel solvent dimethyl sulfoxide/tetrabutylammonium fluoride trihydrate. *Macromolecular Bioscience*, *4*, 1008–1013.
Bashir, S., Critchley, P., & Derrick, P. J. (2001). Use of enzymatic digestion and chemical methylation followed by matrix-assisted laser desorption/ionisation (MALDI) mass spectrometry to sequence a 60 kDa commercial fraction of cellulose acetate. *Cellulose*, *8*, 81–89.
Bax, A., & Davis, D. G. (1985). MLEV-17-based two-dimensional homonuclear magnetization transfer spectroscopy. *Journal of Magnetic Resonance*, *65*, 355–360.
Bax, A., Griffey, R. H., & Hawkins, B. L. (1983). Correlation of proton and nitrogen-15 chemical shifts by multiple quantum NMR. *Journal of Magnetic Resonance*, *55*, 301–315.
Bax, A., & Subramanian, S. (1986). Sensitivity-enhanced two-dimensional heteronuclear shift correlation NMR spectroscopy. *Journal of Magnetic Resonance*, *67*, 565–569.
Braunschweiler, L., & Ernst, R. R. (1983). Coherence transfer by isotropic mixing: Application to proton correlation spectroscopy. *Journal of Magnetic Resonance*, *53*, 521–528.
Dailey, B. P., & Shoolery, J. N. (1955). The electron withdrawal power of substituent groups. *Journal of the American Chemical Society*, *77*, 3977–3981.
Fox, S. C., Li, B., Xu, D., & Edgar, K. J. (2011). Regioselective esterification and etherification of cellulose: A review. *Biomacromolecules*, *12*, 1956–1972.
Ghareeb, H. O., & Radke, W. (2013). Separation of cellulose acetates by degree of substitution. *Polymer*, *54*, 2632–2638.
Goodlett, V. W., Dougherty, J. T., & Patton, H. W. (1971). Characterization of cellulose acetates by nuclear magnetic resonance. *Journal of Polymer Science, A-1: Polymer Chemistry*, *9*, 155–161.
Heinze, T. (1998). New ionic polymers by cellulose functionalization. *Macromolecular Chemistry and Physics*, *199*, 2341–2364.

Heinze, T., Dicke, R., Koschella, A., Kull, A. H., Klohr, E.-A., & Koch, W. (2000). Effective preparation of cellulose derivatives in a new simple cellulose solvent. *Macromolecular Chemistry and Physics*, *201*, 627–631.

Hikichi, K., Kakuta, Y., & Katoh, T. (1995). ^{1}H NMR study on substituent distribution of cellulose diacetate. *Polymer Journal*, *27*, 659–663.

Kamide, K., & Okajima, K. (1981). Determination of distribution of *O*-acetyl group in trihydric alcohol units of cellulose acetate by carbon-13 nuclear magnetic resonance analysis. *Polymer Journal*, *13*, 127–133.

Kay, L. E., Keifer, P., & Saarinen, T. (1992). Pure absorption gradient enhanced heteronuclear single quantum correlation spectroscopy with improved sensitivity. *Journal of the American Chemical Society*, *114*, 10663–10665.

Kim, H., & Ralph, J. (2010). Solution-state 2D NMR of ball-milled plant cell wall gels in DMSO-d_6/pyridine-d_5. *Organic and Biomolecular Chemistry*, *8*, 576–591.

Kim, H., & Ralph, J. (2014). A gel-state 2D-NMR method for plant cell wall profiling and analysis: A model study with the amorphous cellulose and xylan from ball-milled cotton linters. *RSC Advances*, *4*, 7549–7560.

Köhler, S., & Heinze, T. (2007). New solvents for cellulose: Dimethyl sulfoxide/ammonium fluorides. *Macromolecular Bioscience*, *7*, 307–314.

Kono, H. (2013a). Chemical shift assignment of the complicated monomers comprising cellulose acetate by two-dimensional NMR spectroscopy. *Carbohydrate Research*, *375*, 136–144.

Kono, H. (2013b). ^{1}H and ^{13}C chemical shift assignment of the monomers that comprise carboxymethyl cellulose. *Carbohydrate Polymers*, *97*, 384–390.

Kono, H. (2004). Two-dimensional magic angle spinning NMR investigation of naturally occurring chitins: Precise ^{1}H and ^{13}C resonance assignment of α- and β-chitin. *Biopolymers*, *75*, 255–263.

Kono, H., Erata, T., & Takai, M. (2002). CP/MAS ^{13}C NMR study of cellulose and cellulose derivatives. 2. Complete assignment of the ^{13}C resonance for the ring carbons of cellulose triacetate polymorphs. *Journal of the American Chemical Society*, *124*, 7512–7518.

Kono, H., Erata, T., & Takai, M. (2003). Determination of the through-bond carbon–carbon and carbon–proton connectivities of the native celluloses in the solid state. *Macromolecules*, *36*, 5132–5138.

Kono, H., Numata, Y., Erata, T., & Takai, M. (2004). ^{13}C and ^{1}H resonance assignment of mercerized cellulose II by two-dimensional MAS NMR spectroscopies. *Macromolecules*, *37*, 5310–5316.

Lu, F., & Ralph, J. (2003). Non-degradative dissolution and acetylation of ball-milled plant cell walls: High-resolution solution-state NMR. *The Plant Journal*, *35*, 535–544.

Malm, C. J., Tanghe, L. J., & Laird, B. C. (1946). Preparation of cellulose acetate—Action of sulfuric acid. *Industrial and Engineering Chemistry*, *38*, 77–82.

Miyamoto, T., Sato, Y., Shibata, T., Inagaki, H., & Tanahashi, M. (1984). ^{13}C nuclear magnetic resonance studies of cellulose acetate. *Journal of Polymer Science: Polymer Chemistry Edition*, *22*, 2363–2370.

Paul, E. G., & Grant, D. M. (1963). Additivity relationships in carbon-13 chemical shift data for the linear alkanes. *Journal of the American Chemical Society*, *85*, 1701–1702.

Qu, C., Kishimoto, T., Kishino, M., Hamada, M., & Nakajima, N. (2011). Heteronuclear single-quantum coherence nuclear magnetic resonance (HSQC NMR) characterization of acetylated fir (Abies sachallnensis MAST) wood regenerated from ionic liquid. *Journal of Agricultural and Food Chemistry*, *59*, 5382–5389.

Qu, C., Kishimoto, T., Ogita, S., Hamada, M., & Nakajima, N. (2012). Dissolution and acetylation of ball-milled birch (*Betula platyphylla*) and bamboo (*Phyllostachys nigra*) in the ionic liquid [Bmim]Cl for HSQC NMR analysis. *Holzforshung*, *66*, 607–614.

Tezuka, Y., & Tsuchiya, Y. (1995). Determination of substituent distribution in cellulose acetate by means of a ^{13}C NMR study on its propanoated derivative. *Carbohydrate Research*, *273*, 83–91.

Trimbre, L. A., & Bernstein, M. A. (1994). Application of gradients for water suppression in 2D multiple-quantum-filtered COSY spectra of peptides. *Journal of Magnetic Resonance, Series B*, *105*, 67–72.

Xu, D., & Edgar, K. J. (2012). TBAF and cellulose esters: Unexpected deacylation with unexpected regioselectivity. *Biomacromolecules*, *13*, 299–303.

Zhou, Z., Kümmerle, R., Qiu, X., Redwine, D., Cong, R., Taha, A., et al. (2007). A new decoupling method for accurate quantification of polyethylene copolymer composition and triad sequence distribution with ^{13}C NMR. *Journal of Magnetic Resonance*, *187*, 225–233.

Zürcher, R. F. (1967). The cause and calculation of proton chemical shifts in non-conjugated organic compounds. *Progress in Nuclear Magnetic Resonance Spectroscopy*, *2*, 205–257.